Journal of Catalysis **193,** 319–329 (2000)
doi:10.1006/jcat.2000.2903, available online at http://www.idealibrary.com on IDEAL®

Selective Oxidation of *n*-Butane on a V–P–O Catalyst: Improvement of the Catalytic Performance under Fuel-Rich Conditions by Doping

S. Mota,* J. C. Volta,* G. Vorbeck,† and J. A. Dalmon*

*Institut de Recherches sur la Catalyse, 2 Avenue Albert Einstein, 69626 Villeurbanne Cédex, France; and †Haldor Topsoe A/S, Nymollevej, 55 P.O. Box, Lyngby 2800, Denmark

Received January 12, 2000; revised April 24, 2000; accepted April 24, 2000

The oxidation of *n*-butane to maleic anhydride is possible under fuel-rich conditions ($nC_4/O_2 = 0.6$) at 400°C by modifying the vanadium phosphorus oxide (V–P–O) catalysts by doping with Co or Mo; it is impossible on the undoped V–P–O catalyst, which deactivates under the same conditions. The doped precursors were prepared by reduction of the dihydrate $VOPO_4$, $2H_2O$, and dopants were introduced at different moments of the preparation from cobalt acetylacetonate and ammonium heptamolybdate solutions, respectively. The Co-doped V–P–O catalyst (Co/V = 0.77%) conserves a higher capacity for reoxidation of the surface (higher V^{5+}/V^{4+} ratio) and maintains a higher surface distribution of the V, P, and O atoms under fuel-rich conditions: O_2 consumption is not total. Maleic anhydride is then produced and the catalysts do not deactivate. The Mo-doped V–P–O catalysts (Mo/V from 0.88% up to 2.56%) do not give performances as good as those for the Co-doped V–P–O catalyst. It appears that it is necessary to dope at a higher percentage, Mo/V = 2.56%, in order to achieve higher selectivity for MA. The corresponding catalyst is less active (5.3% nC_4 conversion instead of 25.5%) than the Co-doped V–P–O catalyst. This study demonstrates that the nature of the dopant is more important than its way of introduction into the V–P–O matrix. It opens new routes for adapting V–P–O catalysts for oxidizing *n*-butane to maleic anhydride under fuel-rich conditions and for developing new technologies.

Key Words: n-**butane partial oxidation; maleic anhydride; doped V–P–O catalysts; fuel-rich conditions.**

1. INTRODUCTION

The oxidation of *n*-butane to maleic anhydride (MA) on vanadium phosphorus oxides has been the subject of many studies by different groups. Several reviews have been devoted to this catalytic system (1–3). Most of the catalytic investigations and the corresponding physicochemical studies have been done with a high oxygen/*n*-butane ratio (1–3% nC_4/air), usually termed fuel-lean conditions. In this case, a single phase, the vanadyl pyrophosphate $(VO)_2P_2O_7$ is considered as being the active phase of the catalyst. Its microstructure is a key factor in the control of the final catalytic properties by the preparation of its precursor (4, 5). During the activation process under the nC_4-air flow, the $VOHPO_4$, $0.5H_2O$ follows two parallel routes, the dehydration to $(VO)_2P_2O_7$ and the oxidation to $VOPO_4$ phases which are progressively reduced (6). This model has been evidenced by using the complementarity of several techniques which analyze the bulk and the surface properties of the corresponding V–P–O system during the activation process. The XPS study has shown that, under fuel-lean conditions, the V^{5+}/V^{4+} ratio progressively decreases in parallel with the increase of the maleic anhydride yield (6). The positive role of the V^{5+} sites was evidenced by comparing the catalytic activity of a standard $(VO)_2P_2O_7$ catalyst with that of the same $(VO)_2P_2O_7$ catalyst slightly reoxidized (7, 8). From this study, it was concluded that, under fuel-lean conditions, a suitable surface V^{5+}/V^{4+} ratio estimated to be 0.25 corresponded to the improvement of the MA yield observed with the initial reoxidation of the $(VO)_2P_2O_7$ catalyst. The selectivity for MA strongly increased at the early stage of this reoxidation, in parallel with the development of isolated V^{5+} sites in strong interaction with $(VO)_2P_2O_7$. It was previously postulated that the isolated V^{5+} sites should be located in the (100) $(VO)_2P_2O_7$ face (9). For longer oxidation treatments, the development of amorphous V^{5+} microdomains was observed to be detrimental to nC_4 selective oxidation (8). From this study, it was concluded that a suitable oxidizing power (redox state) was necessary for the partial oxidation of n-C_4, in agreement with the industrial DuPont process using the RSR recirculating riser reactor, where the V–P–O catalyst is submitted to periods of reoxidation in a regenerator (10, 11) alternating with periods of interaction with *n*-butane for production of MA by mild oxidation.

When considering the V^{5+}/V^{4+} distribution at the surface of the V–P–O catalyst, it is obvious that the catalytic properties for mild oxidation of *n*-butane will depend on the structural properties of the material, as largely studied, and also on the redox state of the catalyst imposed by the nC_4/O_2 ratio of the gaseous flow, these two aspects being interconnected. A few publications refer to results obtained when working with a high nC_4/O_2 ratio and under

0021-9517/00 $35.00

fuel-rich conditions (12–14). Also, some patents claim interest in such conditions (15, 16). The industrial interest in fuel-rich conditions is due to the fact that maleic anhydride could be recovered without condensing water, as is the case under conventional fuel-lean conditions. But the fuel-rich conditions require a larger catalyst volume since the MA yield in this case would be lower as compared to under fuel-lean conditions (14). However, the main problem is the reduction of the V–P–O catalyst, which affects its performance. In a recent study (17), we have investigated a V–P–O catalyst under fuel-rich conditions in order to develop a new type of reactor based on a ceramic porous tubular membrane. In this reactor, the V–P–O catalyst would be placed as a fixed-bed in the inner volume of the tube and the reactants would be fed separately from both sides of the membrane. Butane would be introduced in the inner volume of the tube, and oxygen would be introduced through the membrane which would act as oxygen distributor along the catalyst bed and thus would maintain a low O_2/C_4 ratio. To simulate the situation of the first layers of the catalyst bed in the membrane reactor (where the O_2/C_4 ratio is the lowest), the work was done, using a conventional microreactor, with a O_2/C_4 ratio of 0.6. For these conditions, a rapid decrease in maleic anhydride production was observed with time. It was associated with reduction of the V–P–O catalyst: the V^{5+} species were either reduced to V^{4+} or masked and/or poisoned by carbonaceous deposits. The reduction was limited to V^{4+} since no signal for V^{3+} species was observed by ^{31}P NMR, spin echo mapping, or XPS. It was concluded that the V–P–O catalyst cannot be used in a membrane reactor without cofeeding oxygen with nC_4 at the inlet of the membrane reactor in order to avoid a total consumption of oxygen and thus to limit total oxidation. In this publication, it was also suggested that these problems should be overcome by the development of the V–P–O catalyst which should result in an improvement of the resistance of the $(VO)_2P_2O_7$ phase toward reduction imposed by the high C_4 concentration under the fuel-rich conditions.

Studies under fuel-rich conditions suggested that the MA yield was improved when the V–P–O catalyst was doped (14–16). In a previous study, under such conditions, it was observed that doping with Co resulted in the production of MA at lower temperature as compared to the undoped V–P–O catalyst. Selectivity is improved by Co doping (18). This was associated with this catalyst's higher susceptibility to oxidation as evidenced, by Raman spectroscopy, with the appearance of the $VOPO_4$ structure at lower temperature during the activation of the corresponding precursor, and by XPS, with a higher V^{5+}/V^{4+} ratio on the final catalyst. It was thus interesting to study the effect of doping by Co under fuel-rich conditions and to compare it with doping by Mo.

In this publication, we study the effect on the resistance to reduction by nC_4 of the V–P–O catalyst modified by Co and Mo doping, under fuel-rich conditions. The preparation implies a vanadium phosphorus oxide catalyst prepared by the reducing preparation route of $VOPO_4, 2H_2O$, termed in a previous publication the "VPD route" (19). Indeed, it was observed that among the different routes of preparation, the VPD route gave the $(VO)_2P_2O_7$ phase with the highest surface platelet morphology exposing preferentially the (100) active plane for maleic anhydride formation.

2. EXPERIMENTAL

2.1. Catalyst Preparation

Two families of doped V–P–O precursors have been prepared using the same route which consists in reduction of $VOPO_4, 2H_2O$ by isobutanol and is termed the VPD route (19). The preparation of $VOPO_4, 2H_2O$ has been previously described (20). The resulting $VOPO_4, 2H_2O$ was recovered by filtration, washed with water, and identified by XRD. Then this solid was refluxed with isobutanol for 21 h, and the resulting blue solid was recovered by filtration and dried in air for 16 h at 110°C. The final solid gives a $VOHPO_4, 0.5H_2O$ precursor denoted "VPD" (19).

For the preparation of the Co-doped VPD precursor, the required mass of the corresponding acetylacetonate salt was dissolved in isobutanol according to the atomic Co/V stoichiometry, prior to the refluxing of the $VOPO_4, 2H_2O$ with the isobutanol solution. The same procedure as for the undoped VPD precursor was followed.

For the preparation of the Mo-doped VPD precursor, a VPD precursor was first recovered after 6 h of refluxing $VOPO_4, 2H_2O$ with isobutanol. Then the VPD precursor was impregnated by an aqueous heptamolybdate solution with the suitable Mo/V ratio. Three MoVPD precursors, denoted VPDMo1, VPDMo2, and VPDMo3, were thus prepared with an increasing Mo/V ratio, following the same procedure. The last MoVPD was prepared differently, according to a modified VPD route: in this case, the heptamolybdate solution was dissolved in isobutanol, the $VOPO_4, 2H_2O$ solid was added with the required Mo/V ratio, and the mixture was refluxed for 16 h. Figure 1 summarizes the preparation of the catalysts.

2.2. Catalyst Activation and Testing

The catalytic experiments were carried out in a fixed-bed reactor at atmospheric pressure as previously described (17). The reactor, a classical tubular Pyrex microreactor, was equipped with a thermocouple inside the catalytic bed for continuous temperature control. Sampling valves were inserted in a hot box heated at 150°C to avoid any condensation of maleic anhydride. The flow of gas reactants was regulated by mass flow controllers. The feed consisted of a mixture of *n*-butane, oxygen, and helium.

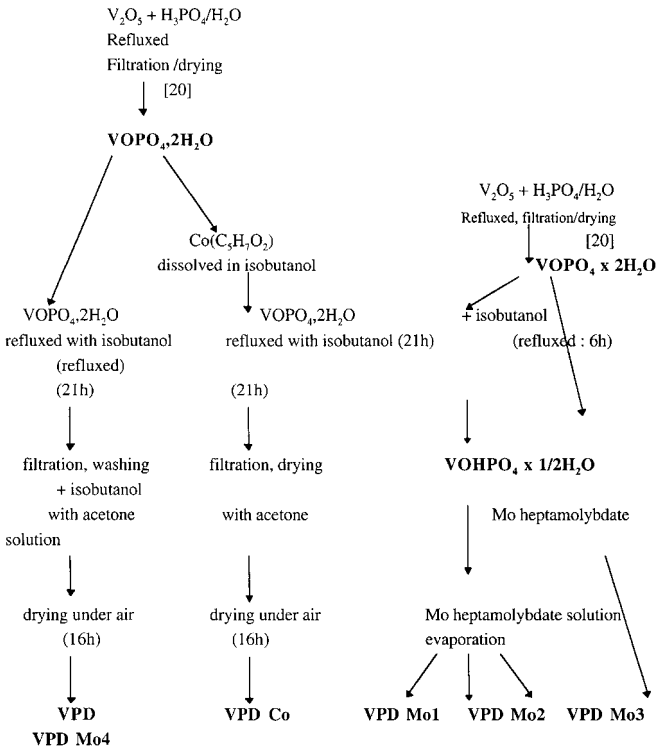

FIG. 1. Synthesis of doped and undoped catalysts.

The VPDCo precursor was activated for 1 h at 390°C under air and then 17 h at 460°C under 1.5% nC_4 in air. The VPDMo precursors were activated for 75 h at 400°C under 1.5% nC_4 in air. The feed consisted of a mixture of *n*-butane, oxygen, and helium. The catalytic reaction was carried out at 400°C under reducing *n*C4-rich conditions (O2/C4 = 0.6) with a constant GHSV of 3000 h^{-1} and the corresponding gas composition: $nC_4/O_2/He = 16.6/10/73.4$. Standard fuel-lean conditions, $O_2/C_4 = 12$, corresponding to $nC_4/O_2/He = 0.8/10/92$, were also used for the initial activating XPS measurements.

Reactants and reaction products were analyzed by on-line gas chromatography using double FID detection (HP5890A series II) with HP-PLOT/Al_2O_3 (C_4H_{10}) and HP-INNOWAX (MA) columns followed by a TCD detector (Intersmat GC IGC 120 MB) with a CTR1 column (O_2, CO, CO_2). A computer was used for integration of the chromatographic peaks with HP Chemstation software.

2.3. Precursor and Catalyst Characterization

The chemical analysis was done by a spectrometer of atomic adsorption (Perkin–Elmer 1100). Solids were dissolved in hydrochloric acid. Measurement of the specific surface area of the catalysts was done by the BET method with volumetric adsorption of N_2 at 77.4 K using a homemade apparatus. X-ray diffraction (XRD) patterns were collected with a Siemens D500 diffractometer using Cu $K\alpha$ radiation.

The ^{31}P nuclear magnetic resonance (NMR) spectra were recorded with a Brucker DSX400 spectrometer, at 161.9 mHz, equipped with a standard 4-mm probe head. The ^{31}P spin echo mapping (SEM) spectra were obtained with a sweep width of 2 mHz, $t = 20$ ms, and 90° pulse length of 1.5 ms. The ^{31}P MAS spectra were recorded at 12 kHz with a P/2 acquisition sequence, a pulse length of 1.5 ms, and a recycle delay of 60 s.

The XPS analysis was performed in a VG Escalab 200R machine using Mg $K\alpha$ radiation. The electrical charge was corrected by setting the binding energy (BE) of adventitious carbon (C_{1s}) at 284.5 eV. For quantitative analysis, we used the integrated area under $V_{2p3/2}$, O_{1s}, P_{2p}, and C_{1s} peaks after smoothing and subtraction of a nonlinear Shirley background. Analysis of the $V_{2p3/2}$ level allowed measurement of the changes in the surface oxidation state of vanadium (V^{5+}, V^{4+}) with a peak decomposition and curve fitting technique, as already described (6).

The catalysts after activation, as previously described, were examined by scanning electron microscopy (SEM) using a Hitachi S800. The atomic composition was measured by X-ray emission spectroscopy (EDX) with a JEOL 840. The depth of examination depends on the elements considered and on the accelerating voltage. It is 0.55 to 1 mm for V, 1.96 to 3 mm for P, 0.34 to 0.6 for Co, and 0.36 to 0.7 for Mo with 20 keV of voltage.

3. RESULTS

Characterization of the activated catalysts (before testing under fuel-rich conditions) is given in Table 1.

For comparison, yield to MA, Y_{MA}, obtained for *n*-butane mild oxidation under fuel-rich conditions ($O_2/C_4 = 0.6$) is given in Fig. 2 for VPD, VPDCo, and VPDMo1 as a function of the time-on-stream (other VPDMo catalysts behave similarly to VPDMo1 in Fig. 2, with only the final yield being slightly affected). In contrast with the VPD catalyst, it appears that at steady state promoted systems produce maleic anhydride after 40 h on stream. This demonstrates the interest of doping V–P–O when catalyzing *n*C4 oxidation under fuel-rich conditions.

TABLE 1

Some Characteristics of the Catalysts after Activation under Standard Conditions

Cat.	Mass percentage (%)				Atomic (%)	
	V	P	Co	Mo	Co/V	Mo/V
VPD	30.32	18.94	—	—	—	—
VPDCo	28.71	17.24	0.27	—	0.77	—
VPDMo1	29.39	18.09	—	0.46	—	0.83
VPDMo2	29.98	19.23	—	0.67	—	1.21
VPDMo3	29.72	19.05	—	1.42	—	2.56
VPDMo4	28.97	28.45	—	0.80	—	1.45

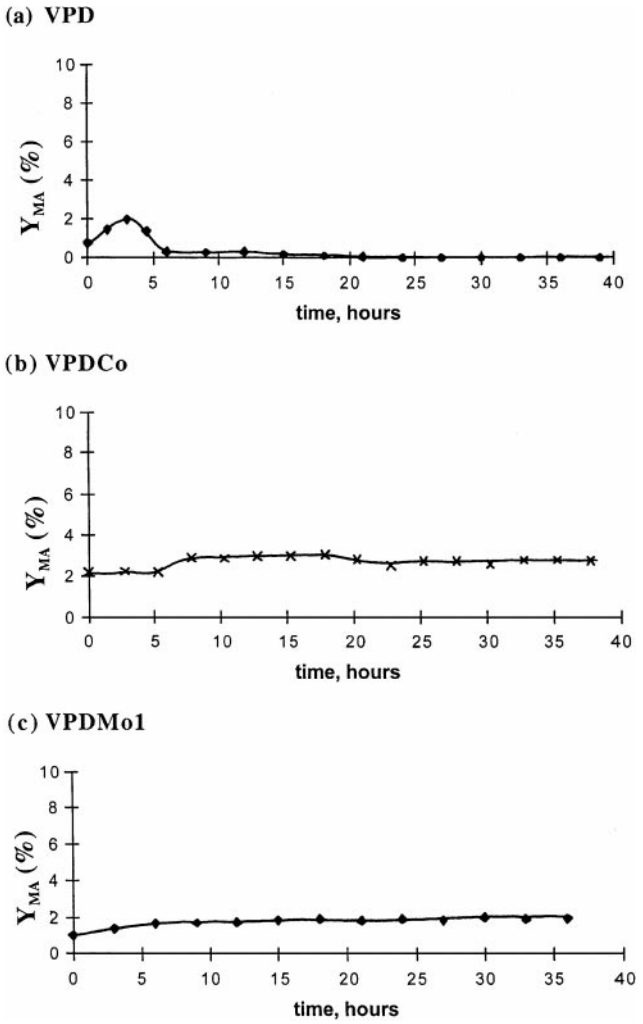

FIG. 2. MA yield for undoped and doped catalysts during the reaction under fuel-rich conditions: (a) VPD, (b) VPDCo, and (c) VPDMo1.

Steady-state catalytic results (after 45 h) are summarized in Table 2. The VPD catalyst converts totally O_2 and the main oxidation products are unsaturated C_4 (S_{C4H8} = 45.1%) and CO (S_{CO} = 32.8%). Maleic anhydride is not produced. CO_2 is observed at a low level (5%), which fits the fact that CO_2 is the fingerprint of the overoxidation of maleic anhydride (17). Cracking catalytic products (17%) are detected due to the reducing feed conditions. The VPDCo catalyst better oxidizes nC$_4$ due to its higher BET area. In this case, the conversion of O_2 is not total (77.9%), which is the main effect of Co doping. Although butenes are produced with almost the same selectivity (42%) as for VPD, the main difference is the production of maleic anhydride with more CO_2 (23.8%) and less CO (22.4%). This is indicative, for the VPDCo catalyst, of the tendency of nC$_4$ oxidation toward MA. This tendency is also confirmed on the VPDMo series for which MA is easily produced with the positive influence of the addition of molybdenum. Note that the effect on the MA selectivity increase is much more pronounced at almost the same level of doping for VPDCo (Co/V = 0.77%, S_{MA} = 11.5%) as compared to VPDMo1 (Mo/V = 0.83%, S_{MA} = 5.7%). However, the nC$_4$ conversion decreases with increased doping by Mo but produces more selective sites for MA production. This is also observed from the increase of the MA intrinsic activity (Table 2).

The surface area of the catalysts was measured after the test. It is given in Table 2. The VPDCo catalyst shows a high surface area (28.0 m^2/g) as compared to the undoped VPD catalyst (17.1 m^2/g), and this appears to be the consequence of the doping effect by cobalt at a low level (Co/V = 0.77%). Let us recall that, in this case, the doped catalyst was prepared by dissolving the Co dopant into the isobutanol reducing solution as acetylacetonate salt, prior to refluxing the $VOPO_4, 2H_2O$ dihydrate (see Fig. 1). The preparation of the VPDMo series follows a different route which consists of an impregnation of the $VOHPO_4, 0.5H_2O$ by a molybdenum heptamolybdate solution. After the test, the BET area of the corresponding Mo catalysts is low, particularly at a low Mo percentage: the BET area is 16.5 m^2/g for VPDMo1, 17.5 m^2/g for VPDMo2, and 21.9 m^2/g for VPDMo3 and does not differ strongly with the VPD catalyst. The percentage of Mo increases in the VPDMo series, as expected from the preparation (Table 1). It is important to note that the route which consists of a dissolution of Mo heptamolybdate into isobutanol prior to refluxing with $VOPO_4, 2H_2O$ gives a catalyst with a very low surface area (6.0 m^2/g), totally inactive for n-butane oxidation.

TABLE 2

Catalytic Results for n-Butane Mild Oxidation under Fuel-Rich Conditions (O_2/C_4 = 0.6) after 45 h on Stream at 400°C

Cat.	Catalytic results (%)							IA (10^{-5} mol · MA · m^{-2} · h^{-1})	S_{BET} ($m^2 \cdot g^{-1}$)
	$C(C_4H_{10})$	$C(O_2)$	S_{MA}	S_{C4H8}	S_{CO}	S_{CO2}	Y_{MA}		
VPD	15.5	100	0	45.1	32.8	5	0	0	17.1
VPDCo	25.5	77.9	11.5	42	22.4	23.8	2.9	4.62	28.0
VPDMo1	16	96.5	5.7	47.2	26.6	20.5	0.9	1.28	16.5
VPDMo2	8.2	81	8.3	33.7	30.7	27.3	0.7	1.34	17.5
VPDMo3	5.3	63.2	36.5	1.1	28.8	33.8	1.9	3.25	21.9

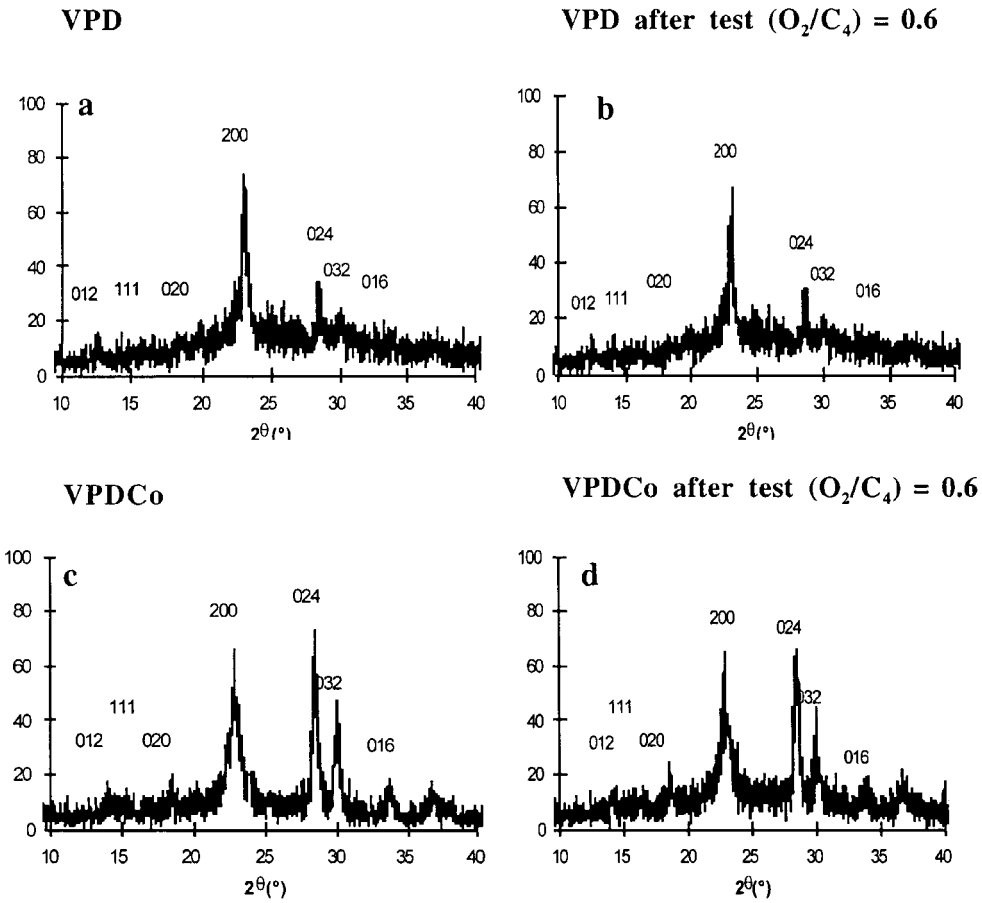

FIG. 3. XRD spectra of undoped and Co-doped VPD catalysts: (a) VPD activated, (b) VPD after test under fuel-rich conditions, (c) VPD Co activated, and (d) VPD Co after test under fuel-rich conditions.

The XRD spectra of the activated VPD (a) and equilibrated VPD (b) after test under fuel-rich conditions are given in Fig. 3, simultaneously with those of the corresponding activated (c) and equilibrated (d) VPDCo catalysts. All spectra are similar and characteristic of the $(VO)_2P_2O_7$ phase with a broadening of the (200) reflection, typical of the well-known VPD morphology which develops platelets with [100] normal (19). The XRD spectra of the VPDMo series are given in Fig. 4 for the activated catalysts and in Fig. 5 for the VPDMo catalysts after test under reducing conditions. They are also characteristic of the VPD type morphology. The XRD spectrum of the activated VPDMo4 catalyst (Fig. 4d) can be indexed as a mixture of different $VOPO_4$ phases (α_{II}-, γ-, δ-$VOPO_4$, and $VOPO_4$, $2H_2O$) with their characteristic lines. The presence of these V^{5+} phases can explain the poor performance of the corresponding catalyst (Table 2).

The activated VPD (a), VPDCo (b), and VPDMo3 (d) catalysts were examined by SEM (Fig. 6). Sand-rose platelets were observed for the three catalysts. Their sizes were smaller for the activated VPDCo catalyst, which should be correlated with the higher BET area observed after the catalytic test for the corresponding catalyst. Platelets appeared more eroded, with a lozenge shape, and curved. For the activated VPDMo catalysts, the same type of morphology was observed.

Table 3a shows the EDX results obtained on the activated VPD, VPDCo, and VPDMo3 catalysts. EDX results are given in parentheses for comparison with the XPS results. There are almost no differences with the XPS results if we take into account, for EDX, the contribution of C, which cannot be detected by EDX, since C is deposited for the EDX examination but measured by XPS.

Figure 7 presents the ^{31}P NMR spin echo mapping spectra of the activated VPD, VPDCo, and VPDMo catalysts. While the activated VPD catalyst (Fig. 7a) shows a spectrum typical of only the $(VO)_2P_2O_7$ phase (essentially one signal at 2495 ppm), the activated VPDCo catalyst (Fig. 7b) shows, in addition to the signal of $(VO)_2P_2O_7$, signals near 0 ppm, typical of V^{5+} species, and in the 1000 ppm range, typical of V^{4+}–V^{5+} dimers, which is indicative of a more oxidized situation due to the effect of the Co dopant on vanadium sites. The progressive increase of the oxidation state of vanadium for the VPDMo activated catalysts (Figs. 7c,

TABLE 3a

XPS Results on Activated Catalysts (for Activation Conditions, See Paragraph 2.2)

	Atomic surface distribution (%)							V (%)		
Activated cat.	V	Na	P	O	C	Doping metal	P/V	V^{4+}	V^{5+}	V^{5+}/V^{4+}
VPD	10.7 (15.7)	(4.5)	17.3 (15.3)	65.7 (64.2)	6.3	—	1.62	65.8	35.2	0.53
VPDCo	11.3 (14.5)	(2.1)	17.6 (15.1)	65.7 (65.2)	5.3	0.18	1.56	68.7	31.3	0.46
VPD Mo1	10.2		17.4	69.0	3.2	0.18	1.70	72	28	0.39
VPD Mo2	10.1		16.6	67.0	6.0	0.28	1.64	70	30	0.42
VPD Mo3	9.8 (14.3)	(4.5)	16.5 (14.9)	67.3 (64.9)	6.0	0.48	1.68	66	34	0.52

Note. EDX results are given in parentheses for comparison with XPS results.

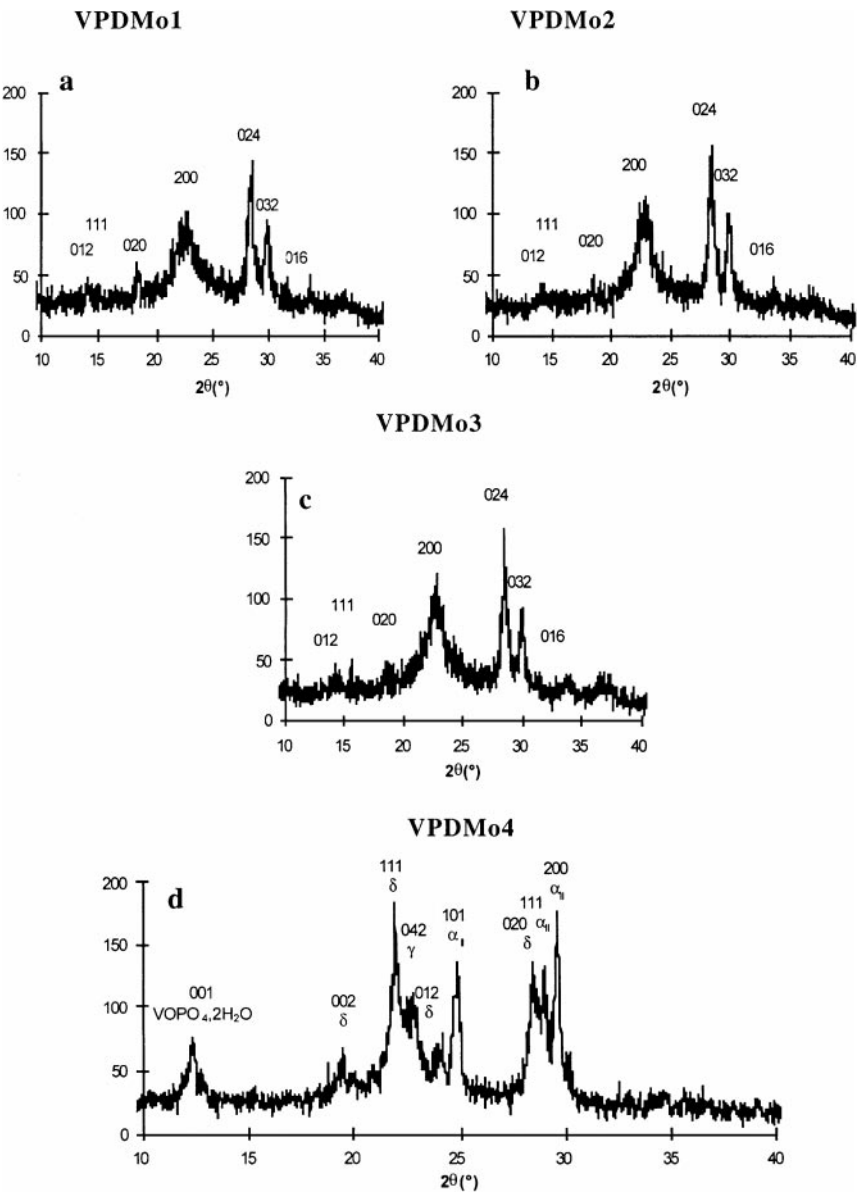

FIG. 4. XRD spectra of fresh doped VPD Mo catalysts (activated): (a) VPD Mo1, (b) VPD Mo2, (c) VPD Mo3, and (d) VPD Mo4.

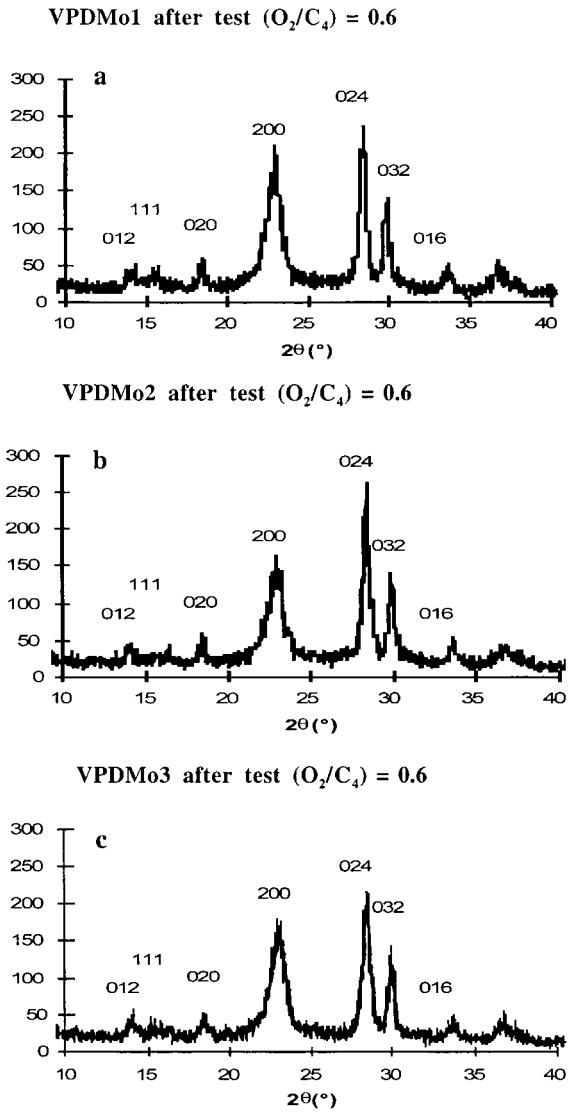

FIG. 5. XRD spectra of doped VPD Mo catalysts after test under fuel-rich conditions: (a) VPD Mo1, (b) VPD Mo2, and (c) VPD Mo3.

7d, and 7e) with increasing percentage of the Mo dopant is obvious from the increase of the contributions near 0 and at 1000 ppm. The quasi-absence of $(VO)_2P_2O_7$ and the presence of only $VOPO_4$ phases is confirmed from the spectrum of the activated VPDMo4 catalyst (Fig. 7f). Figure 8 gives the ^{31}P NMR spin echo mapping spectra of the VPD (a), VPDCo (b), and VPDMo (c, d, and e) equilibrated catalysts after the test under reducing conditions ($nC_4/O_2 = 0.6$). Figure 8 shows that the catalytic reducing treatment has consumed most of the V^{5+} species and the V^{4+}–V^{5+} dimers. A slight signal near 0 ppm is, however, observed for the doped catalysts, which indicates that the catalysts have still conserved an oxidative capacity. This will be confirmed by the XPS study. The displacement at a higher position of the signal of vanadium pyrophosphate for the VPDMo series (2610–2640 ppm) is indicative that this doping procedure has favored the reorganization of the corresponding materials during the test under fuel-rich conditions.

Tables 3a and 3b compare the XPS results between the catalysts activated under fuel-lean conditions (a) (see Subsection 2.2) and the catalysts after the test under fuel-rich conditions (b). The atomic surface distribution shows comparable results for all the activated catalysts (Table 3a). Note that the percentage of surface oxygen atoms is high (64–66%). The doping elements (Co and Mo) are detected as expected. Note also the usual increased P/V ratio (1.60–1.70), as generally observed for the V–P–O catalysts working toward nC_4 oxidation under fuel-lean conditions. The V^{5+}/V^{4+} ratio for these catalysts as calculated from the deconvolution of the $V_{2p3/2}$ levels of V^{4+} and V^{5+} observed at 516.9 and 518.0 eV, respectively (20), shows a value around 0.4–0.5, usually observed for V–P–O catalysts working toward nC_4 oxidation under fuel-lean conditions. Some carbon is detected, which can be produced by contamination from carbonaceous species coming from the nC_4/O_2 atmosphere of activation of the precursors.Very different information is observed from the atomic surface distribution after the test under reducing conditions ($O_2/C_4 = 0.6$) (Table 3b). Results will be discussed with reference to the same catalysts activated under fuel-lean conditions:

—For VPD, the V^{5+}/V^{4+} ratio has also strongly decreased (from 0.53 down to 0.19). A strong increase of C is also observed (from 6.3 up to 55.6%). V, P, and O have considerably decreased. Note also that the P/V ratio has increased (from 1.62 to 2.06) This should correspond to a higher acidity of the corresponding catalysts.

TABLE 3b

XPS Results on the Catalysts: After Test under Fuel-Rich Conditions ($O_2C_4 = 0.6$)

	Atomic surface distribution (%)						V (%)			
Equilibrated cat.	V	P	O	C	Doping metal	P/V	V^{4+}	V^{5+}	V^{5+}/V^{4+}	$V^{5+} \times V_{Total}$
VPD	3.1	6.4	34.9	55.6	—	2.06	84	16	0.19	0.496
VPDCo	9.2	15.3	62.9	12.4	0.2	1.66	74	26	0.35	2.392
VPDMo1	4.9	10.0	43.0	41.9	0.15	2.04	89	11	0.12	0.539
VPDMo2	6.0	11.2	47.7	34.8	0.18	1.86	86	14	0.16	0.840
VPDMo3	9.0	15.3	55.8	19.5	0.38	1.69	79	21	0.27	1.890

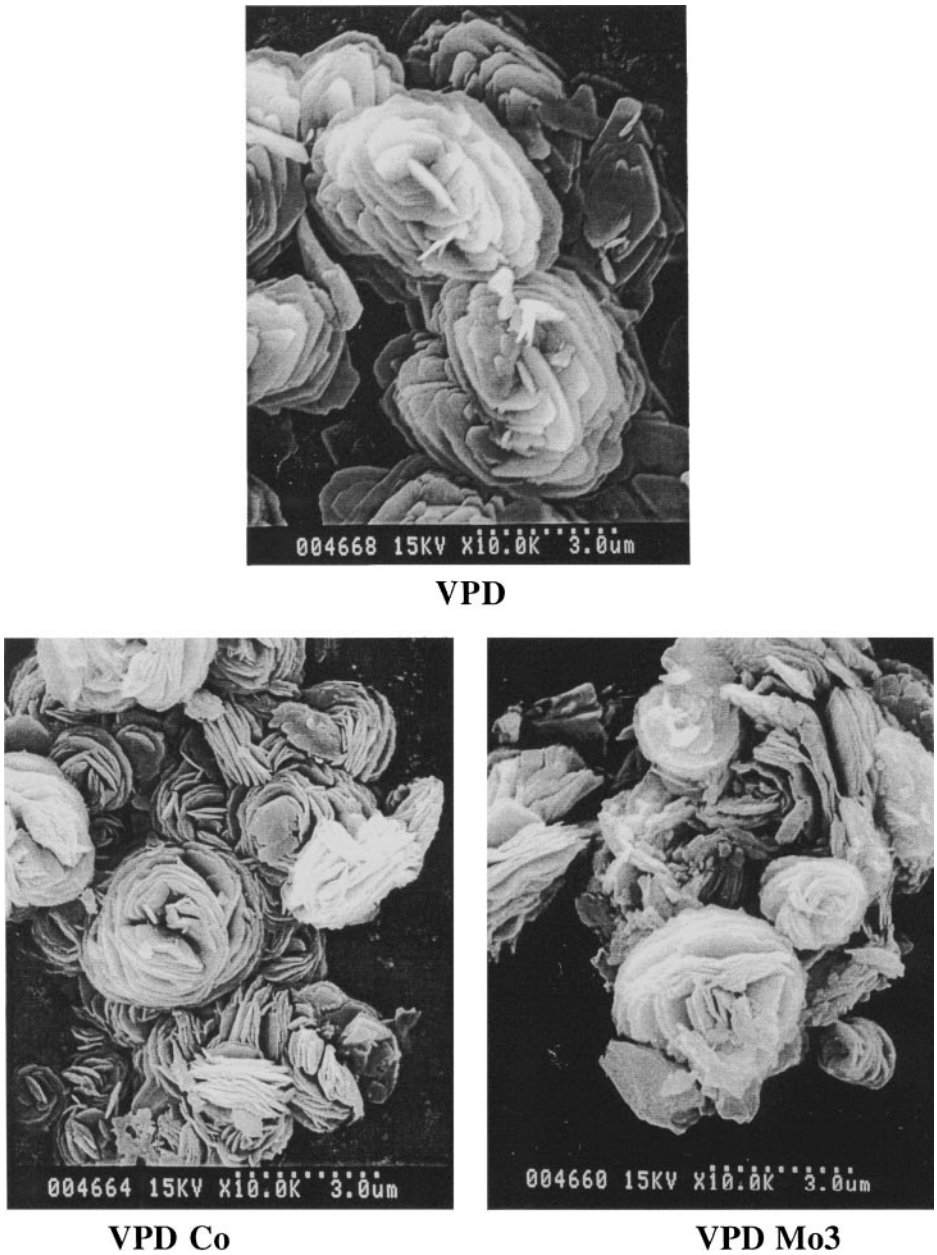

FIG. 6. SEM examinations of the activated catalysts.

—For VPDCo, the V^{5+}/V^{4+} ratio (0.35) is clearly higher than that for VPD (0.19). The masking effect of C is much less pronounced, and values not so far from the values observed on the corresponding activated VPDCo catalyst are observed: 9.2% (b) for V as compared to 11.3% (a), 15.3% (b) for P as compared to 17.6% (a), and 62.9% (b) for O as compared to 65.7% (a). The C percentage (12.4%) is not so high as compared to that of VPD (55.6%). The P/V ratio (1.66) approaches the values observed for the C_4 fuel-lean conditions of catalysis (1.56).

—For VPDMo1, the V^{5+}/V^{4+} ratio is low (0.12). The C (41.9%) masking effect appears on V (4.9%), P (10.0%), and O (43%). The P/V ratio is still high (2.04). When doping with more Mo, for VPDMo2 and VPDMo3, the atomic surface distribution approaches that of VPDCo, without reaching it, however: 9.0% for V, 15.3% for P, 55.8% for O, and 19.5% for C for VPDMo3.

4. DISCUSSION

In a previous publication (17), we have shown that vanadium phosphorus oxide cannot be used for a long time on stream as a catalyst for *n*-butane oxidation to maleic anhydride (MA) under fuel-rich conditions ($C_4/O_2 = 0.6$): the

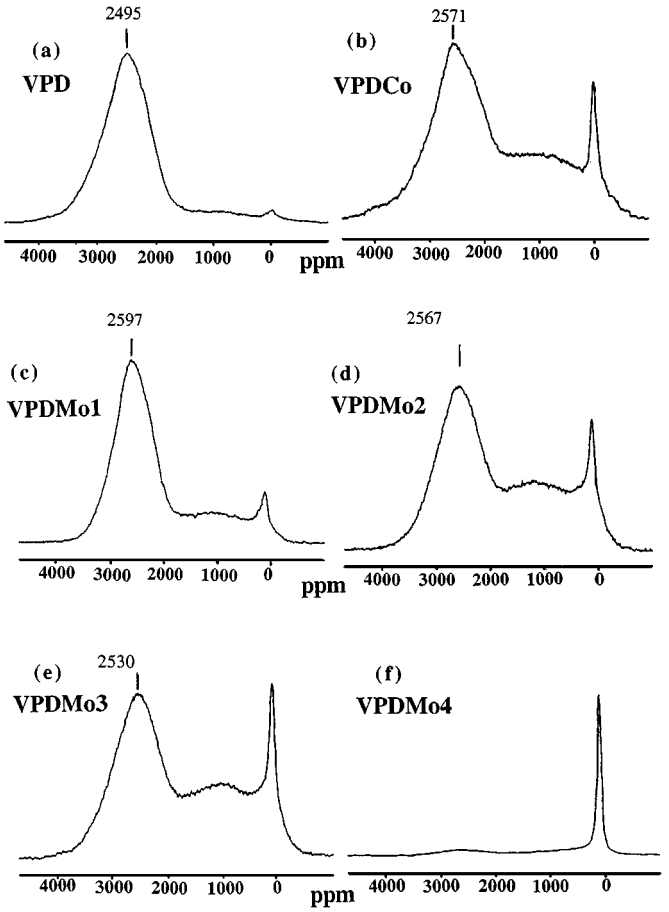

FIG. 7. The ^{31}P (SEM) NMR spectra of the activated undoped and doped VPD catalysts: (a) VPD, (b) VPD Co, (c) VPD Mo1, (d) VPD Mo2, (e) VPD Mo3, and (f) VPD Mo4.

V–P–O catalyst produces MA for a very short period and consumes all oxygen in the feed. At this moment CO is mainly produced with almost no CO_2. It was concluded that CO formation occurs mainly by the oxidation of adsorbed *n*-butane whereas CO_2 is formed by the overoxidation of maleic anhydride. In the present publication, we improve the oxidizing capacity of the V–P–O catalyst, and we show that it is possible to limit the deactivation under fuel-rich conditions by modifying the vanadium phosphorus oxide catalyst by doping with Co or Mo.

The reference VPD type catalyst shows, under fuel-rich conditions ($O_2/C_4 = 0.6$), a total consumption of O_2 in the feed. This is associated with the nonproduction of maleic anhydride on this catalyst (Fig. 2 and Table 2), as previously observed on the V–P–O type catalyst (17). The deactivation of the vanadium phosphorus oxide catalyst is thus observed under fuel-rich conditions independently of the morphology of the $(VO)_2P_2O_7$ crystals. The V–P–O material does not suffer from the high reducing conditions of the test: this corresponds to a decrease of the V^{5+}/V^{4+} ratio and a P/V increase as observed by XPS (Tables 3a and 3b). This favors the production of unsaturated C_4 and the total oxidation to CO rather than to CO_2. Carbon then covers the surface of the catalyst, masks V and P, and limits the accessibility to oxygen.

The Co-doped VPD catalyst avoids such poor behavior under fuel-rich conditions. Indeed, the oxidizing power of cobalt on vanadium is obvious from the ^{31}P NMR spin echo mapping spectrum of the corresponding activated catalyst, which shows the increase of the signals associated with V^{5+} species (Fig. 7b). If most of the bulk V^{5+} species are consumed under fuel-rich conditions (as observed by NMR, Fig. 8), the oxidizing capacity of the VPDCo catalyst is obvious from the high atomic surface V^{5+}/V^{4+} ratio (0.35) as well from the high atomic surface distribution for V, P, and O (Table 3b). All XPS analysis information on this catalyst under fuel-rich conditions approaches the XPS analysis information on the same catalyst under fuel-lean conditions: Co retains the active O species for the production of MA in the vicinity of the V and P active species of the catalyst.

The catalysts of the VPDMo, series, Mo-doped VPD catalysts, show a behavior of the same type under fuel-rich catalytic conditions, but a significant production of MA

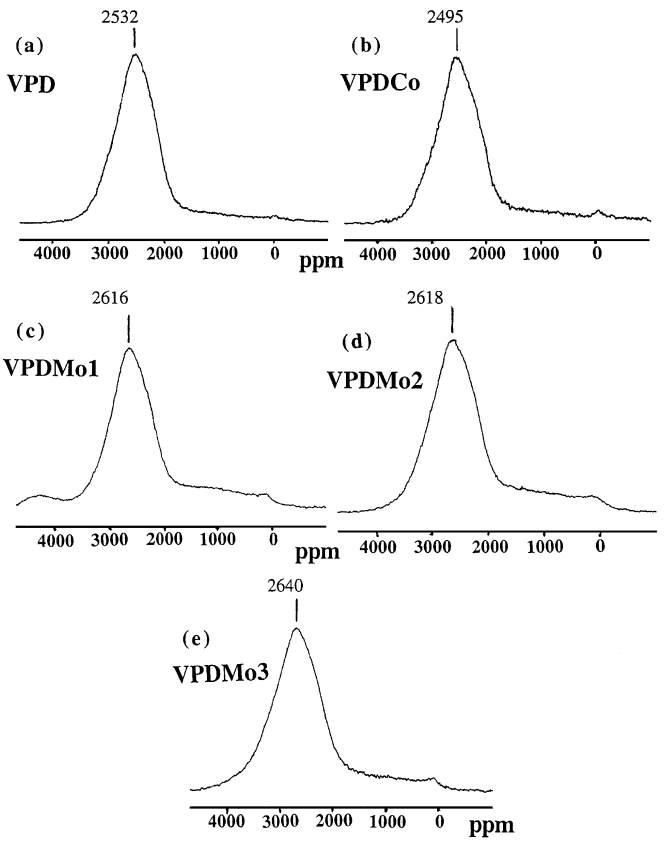

FIG. 8. The ^{31}P NMR (SEM) spectra of undoped and doped catalysts after test under fuel-rich conditions ($O_2/C_4 = 0.6$): (a) VPD, (b) VPD Co, (c) VPD Mo1, (d) VPD Mo2, and (e) VPD Mo3.

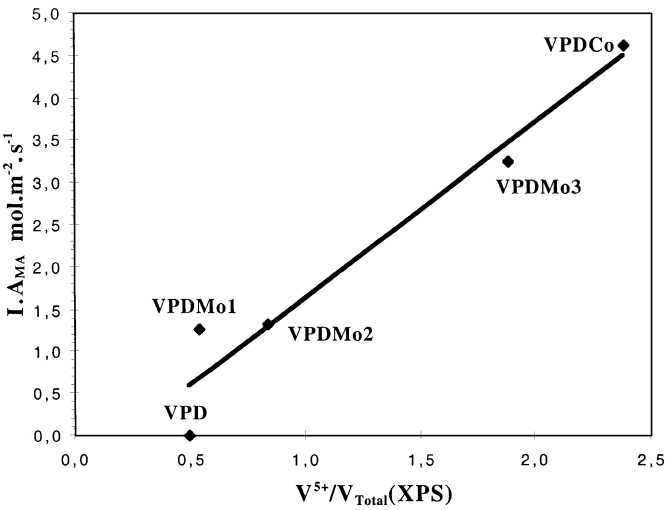

FIG. 9. Correlation between MA intrinsic activity and XPS results.

is observed for doping at the higher level Mo/V = 2.56% as compared to Co/V = 0.77%. The catalysts are, however, much less active. The differences observed can be explained by the different methods of preparation. As a matter of fact, Co dopant has been dispersed in the V–P–O matrix at the stage of the preparation of the corresponding precursor in organic medium. The different method of doping of the $VOHPO_4, 0.5H_2O$ precursor by impregnation by the Mo heptamolybdate solution should explain the difference observed between the Mo- and Co-doped VPD catalysts.

In a previous publication (21), we established a correlation for a series of doped and undoped V–P–O catalysts between the MA intrinsic activity and the contribution of the V^{4+}–V^{5+} dimers (measured by ^{31}P NMR by spin echo mapping in the 200–1500 ppm range) for *n*-butane oxidation under fuel-lean conditions ($nC_4/O_2/He = 1.5/18.5/80$, $T = 430°C$, $GSHV = 1000\ h^{-1}$). It was observed by ^{31}P NMR (compare Figs. 7 and 8) that most of the V^{5+} species (bulk as identified by this technique) are consumed under *n*-butane fuel-rich oxidation conditions, but that a slight contribution of these species was still present. XPS was used to detect these species and to make correlations with the catalytic results. A correlation is observed, Fig. 9, for the catalysts of the two series and VPD between the maleic anhydride intrinsic activity, IA_{MA} (see Table 2) and the surface V^{5+} species (measured by $\%V^{5+} \times V_{XPS}$). It should thus be concluded that for nC_4 oxidation under fuel-rich conditions, the MA production depends on the superficial density of V^{5+} sites which should be restricted to the surface. It appears clearly that the higher the V^{5+}/V^{4+} XPS ratio, the lower the carbon deposition. For the unpromoted VPD, the V^{5+} species are reduced, leading to dehydrogenation reaction, originating the formation of carbonaceous species.

5. CONCLUSIONS

The main objective of this study was to develop a vanadium phosphorus oxide catalyst able to work under fuel-rich conditions for *n*C4 mild oxidation. This study has demonstrated that doping with Co or Mo leads to such a promoting effect. We have observed that the nature of the doping element is more important than its way of introduction in the V–P–O catalyst. Co as dopant has more oxidizing power on the V–P–O system than Mo: it favors a higher V^{5+}/V^{4+} ratio under fuel-rich oxidation conditions, limits the C deposition, and makes possible the production of maleic anhydride on this modified V–P–O system.

This study opens a new route for the development of a new type of reactor based on a ceramic porous tubular membrane for which the chemical composition of the V–P–O catalyst will be adjusted to be adapted to reducing *n*C4/O2 catalytic conditions at the inlet of the membrane reactor. Indeed, besides the choice of a proper membrane, membrane reactors may also need a specifically designed catalyst adapted to their catalysis conditions (22). Studies are underway for optimization of these systems and especially to define the best method for dopant introduction.

ACKNOWLEDGMENTS

This work was conducted in the framework of the Contract Brite BRPR-CT955-0046. The authors are indebted to the support of the European Community. We gratefully acknowledge Dr. Khadija Aït Lachgar for her help in the preparation of one V–P–O precursor, Dr. P. Delichère and M. Brun for XPS analysis, M.C. Durupty for ^{31}P NMR, and V. Martin for SEM and EDX examination of the catalysts.

REFERENCES

1. Hodnett, B. K., *Catal. Rev. Sci. Eng.* **27**, 373 (1985).
2. Centi, G., Trifiro, F., Ebner, J. B., and Franchetti, V. M., *Chem. Rev.* **88**, 55 (1988).
3. Cavani, F., and Trifiro, F., *Catalysis* **11**, 246 (1994).
4. Duvauchelle, N., and Bordes, E., *Catal. Lett.* **57**, 81 (1999).
5. Ellison, I. J., Hutchings, G. J., Sananés, M. T., and Volta, J. C., *J. Chem. Soc. Chem. Commun.*, 1093 (1994).
6. Abon, M., Béré, K. E., Tuel, A., and Delichère, P., *J. Catal.* **156**, 28 (1995).
7. Aït Lachgar, K., Abon, M., and Volta, J. C., *J. Catal.* **171**, 383 (1997).
8. Aït Lachgar, K., Tuel, A., Brun, M., Herrmann, J. C., Kraft, J. M., Martin, J. R., Volta, J. C., and Abon, M., *J. Catal.* **177**, 224 (1998).
9. Volta, J. C., Béré, K. E., Zhang, Y. J., and Olier, R., *in* "ACS Symposium Series, 523" (S. T. Oyama and J. W. Hightower, Eds.), p. 217. Am. Chem. Soc., Washington, DC, 1993.
10. Contractor, R. M., Bergna, H. E., Chowdry, U., and Sleight, A. W., *in* "Fluidization VI" (J. R. Grace, L. W. Shemilf, and M. A. Bergougnou, Eds.), p. 589. Engineering Foundation, New York, 1989.
11. Contractor, R. M., Garnett, D. I., Horowitz, H. S., Bergna, H. E., Patience, G. S., Schwartz, J. T., and Sisler, G. M., *in* "New Developments in Selective Oxidation II" (V. Cortés Corberan and S. Bellon, Eds.), p. 233, Elsevier, Amsterdam, 1994.
12. Centi, G., Fornasari, G., and Trifiro, F., *J. Catal.* **89**, 44 (1984).
13. Centi, G., Fornasari, G., and Trifiro, F., *Ind. Eng. Chem. Prod. Res. Dev.* **24**, 32 (1985).

14. Hutchings, G. J., *Appl. Catal.* **72**, 1 (1991).
15. Higgins, R., and Hutchings, G. J., U.S. Patent 4222945 (1980). [Assigned to Imperial Chemical Industries]
16. Higgins, R., and Hutchings, G. J., U.S. Patent 4317777 (1982). [Assigned to Imperial Chemical Industries]
17. Mota, S., Abon, M., Volta, J. C., and Dalmon, J. A., *J. Catal.* **193**, 308 (2000).
18. Ben Abdelouahab, F., Olier, R., Ziyad, M., and Volta, J. C., *J. Catal.* **157**, 687 (1995).
19. Kiely, C. J., Burrows, A., Sajip, S., Hutchings, G. J., Sananés, M. T., Tuel, A., and Volta, J. C., *J. Catal.* **162**, 31 (1996).
20. Sananés-Schulz, M. T., Ben Abdelouahab, F., Hutchings, G. J., and Volta, J. C., *J. Catal.* **163**, 346 (1996).
21. Sananés-Schulz, M. T., Tuel, A., Hutchings, G. J., and Volta, J. C., *J. Catal.* **166**, 388 (1997).
22. Dalmon, J-A., "Handbook of Heterogeneous Catalysis" (G. Ertl, H. Knözinger, and J. Weitkamp, Eds.), Chap. 9.3, pp. 1387–1398. VCH, Weinheim/New York, 1997.